Seismic damage assessment of precast reinforced concrete buildings based on monitoring data

Laura Ierimonti [a], Ilaria Venanzi [a], Filippo Ubertini [b], Annibale Luigi Materazzi [b]
[a] *Department of Civil and Environmental Engineering, University of Perugia, Via G. Duranti, 06125, Perugia, Italy*
E-mail: laura.ierimonti@unipg.it, ilaria.venanzi@unipg.it, filippo.ubertini@unipg.it, materazzi@unipg.it

Keywords: Precast reinforced concrete structures; continuous dynamic monitoring; earthquake-induced damage detection; nonlinear analysis.

ABSTRACT
Major earthquakes that occurred during the last decades in central Italy revealed a significant vulnerability of precast industrial and commercial reinforced concrete (RC) buildings, which involves both structural and non-structural components.
In this context, a post-earthquake methodology for the rapid diagnosis of the structural safety based on structural health monitoring techniques is proposed for precast RC structures, with a twofold role: the capability of detecting possible damages after a seismic event and the prevention of the damage accumulation over time by tracking the structural dynamic characteristics.
In order to validate the methodology, a Finite Element Model (FEM) is built to simulate the response of the structure under different seismic inputs and to identify the most damage-sensitive areas within the building. To this aim, a continuous monitoring system consisting of accelerometers and inclinometers is designed and experimentally tested, with the main scope of integrating it at the top and at the bottom of some suitable selected building's columns. Subsequently, results of nonlinear static and dynamic analyses are used to probabilistically define the seismic vulnerability of the building by selecting proper alert states as a function of damage indicators based on peak displacements. Hence, alert states are included in fragility curves, numerically reconstructed for the drift-dependent damage states, which allow to account for the uncertainties involved in the problem, such as those associated to the variability of the seismic load and to the structural characteristics. Finally, a simulated continuous monitoring is used to track in time the potential achievement of an alert state for the specific damage state, allowing the real-time post-earthquake diagnosis of the structural safety conditions.

1 INTRODUCTION

During the last decades precast reinforced concrete technology has represented a widely used construction method, especially adopted for industrial and commercial buildings. Recently, existing precast structures experienced several seismic-induced damages (Liberatore et *al*. 2013), revealing a significant vulnerability which can be also related to the low level of hyperstaticity (Belleri et *al*. 2014). Different damage scenarios are also revealed by shaking table tests (Senel and Kayhan 2010, Guo et al. 2019). Indeed, considering the collapse mechanisms, it emerges that particular attention must be devoted to the connection systems between the various precast elements (Arango et *al*. 2018, Brunesi and Nascimbene 2017). Hence, if on the one hand a proper design is crucial for the building safety and for the prevention of structural and non-structural damages, on the other hand it can be suitable to consider structural health monitoring (SHM) systems (Isidori et *al*. 2016). Long-term SHM is already used in real-world historical masonry structures (Ubertini et *al*. 2018) and also in other types of structures (such as bridges, school buildings and more) in order to track their dynamic characteristics over time with the main objective of highlighting possible damage after an earthquake. In this context, the benefits of SHM can also be exploited for precast RC buildings (Pierdicca et *al*. 2016, Belleri et al. 2014), a field that is currently quite unexplored.

The present research work aims at implementing a methodology for the rapid post-earthquake damage assessment of precast RC industrial buildings, by means of continuous monitoring data.

Preliminary nonlinear static analyses (NLSA) and nonlinear dynamic analyses (NLDA) are carried out on a FEM of a precast RC structure in order to relate the response in terms of interstory

drift ratio (IDR) to the level of damage experienced by the structure, probabilistically defined.

The continuous monitoring activity is simulated by applying to the FEM a real seismic sequence and the results are compared to the alert thresholds in order to perform real-time post-earthquake diagnosis of the system.

2 GENERAL METHODOLOGY

2.1 The proposed methodology

The aim of the proposed approach is to provide a real-time diagnosis tool for precast RC structures, by making use of long-term monitoring data. A schematic representation of the methodology is summarized in Figure 1.

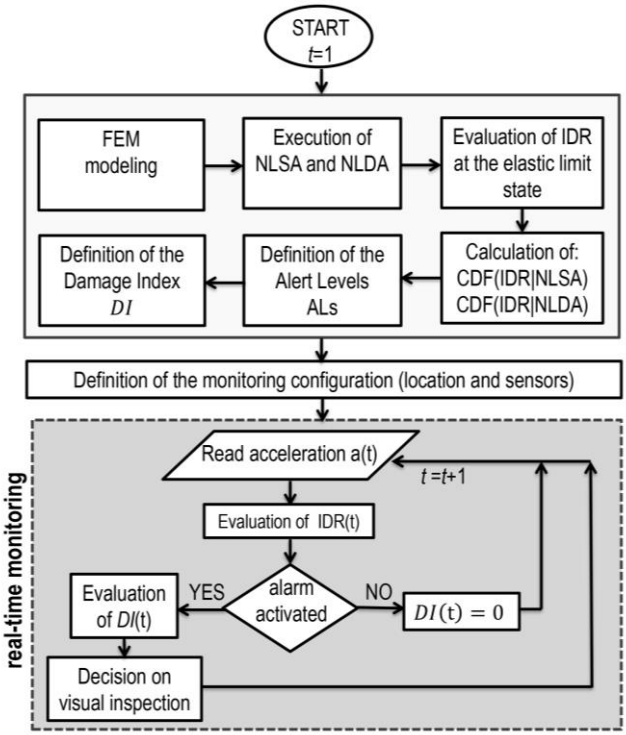

Figure 1: Block diagram illustrating the methodology flowchart.

As illustrated in Figure 1, the methodology can be globally divided in two main parts: offline preliminary analyses and the real-time monitoring. The flowchart representing the offline activity is characterized by the following steps:

- Build a FEM of the structure.
- Perform NLSA by computing the capacity curves;
- Perform NLDA by selecting a set of multi-component spectrum-compatible accelerograms.
  In order to account for the uncertainties related to the characterization of the seismic action and facilitating a probabilistic-based approach, different analysis cases are considered: for the two principal building's directions, for different distributions of lateral forces, for different locations of the conventional accidental mass eccentricity and for different reference joints.
- Use results of NLSA and NLDA, separately, to compute for each analysis case the values of the IDR for which plastic hinges at the columns base are activated.
- Use the results of NLSA and NLDA for computing the cumulative distribution function (CDF) of the IDRs corresponding to the elastic threshold (first plastic hinge formation).
- Define the Alarm Levels (ALs) for the on-off control.
- Define the Damage Index (*DI*).
- Decide for the monitoring configuration within the structures, i.e., types of sensors and their optimal location.

The real-time activity is an on-off control which consists in the evaluation of the alert state of the structure during and post an earthquake. It is based on recorded data and preliminary analyses results. This phase is characterized by the following steps:

- Read the acceleration $a(t)$ available from the data recorded by the installed sensors.
- Evaluate the IDR(t) by double numerical integration.
- If IDR(t) assumes values exceeding the selected ALs, the alarm is activated, the *DI*(t) is computed and, consequently, decisions on the occupants safety are taken accompanied by visual inspections. Otherwise *DI*(t) assumes zero values (an undamaged condition is inferred).

2.2 Alarm levels

For the definition of the ALs it is assumed that the main risky damage limit state concerns the first plastic hinge formation at the column base. Indeed, generally, in precast RC industrial buildings, constraints between structural elements are hinges,

except for joints at the base of the columns that are fixed. Without loss of generality, several types of limit states could be easily considered in the procedure like those associated to the sliding of joints between beams and the top ends of the columns or damage to nonstructural elements (Ierimonti et al. 2017).

According to the general methodology presented in Section 2.1, in order to distinguish between different alert ranges, the probability distributions of IDR separately obtained from NLSA and NLDA are considered. The following ALs, function of the mean value μ_d and of the standard deviation σ_d, are defined:

1. Alert Level 1 (AL1): $\mu_d - 1.65\sigma_d$ (90% of the confidence interval);
2. Alert Level 2 (AL2): μ_d

Consequently the on-off control can be considered as:

1. alarm inactive: below AL1.
3. alarm active: above AL2.

2.3 The damage index

In order to quantify the structural damage, a structural damage index is considered (Graham and Rakesh 1988):

$$\mathrm{DI}_{\mathrm{IDR}}(t) = \frac{\mathrm{IDR}_c(t) - \mathrm{IDR}_t}{\mathrm{IDR}_u - \mathrm{IDR}_t} \quad (1)$$

where $\mathrm{IDR}_c(t)$ is the IDR value calculated at time *t*, IDR_t is the threshold value, IDR_u is the ultimate value. The $\mathrm{DI}_{\mathrm{IDR}}(t)$ changes with time and it assumes: zero values if the $\mathrm{IDR}_c(t) < \mathrm{IDR}_t$, implying no damage; unit value if the failure is reached ($\mathrm{IDR}_c(t) = \mathrm{IDR}_u$); values between 0 and 1 depending on the level of damage within the AL. Since the limit state chosen concerns the first plastic hinge formation at the column base, IDR_u is assumed equal to the elastic limit state corresponding to the Alert Level 2 (μd), assumed as the mean value of the IDR distribution. The threshold value IDR_t is assumed as the value corresponding to the Alert Level 1. Consequently, Eq. (1) becomes:

$$\mathrm{DI}_{\mathrm{IDR}}(t) = \frac{\mathrm{IDR}_c(t) - \mu_d + 1.65\sigma_d}{1.65\sigma_d} \quad (2)$$

2.4 The monitoring system

The proposed methodology presented in Section 2 required a monitoring system able to measure the interstory drift. One of the most common methods for structural health monitoring is the use of accelerometers that can be easily employed to determine dynamic displacements through double signal integration during an earthquake. One possible configuration, experimentally tested by the Authors, is:

- 1 bidirectional accelerometer at the top and 1 bidirectional accelerometer at the bottom of the most damage-sensitive columns that can be used to evaluate by integration the relative dynamic displacement (IDR);
- 1 inclinometer to estimate possible residual displacements, not detectable through accelerometers.

The accelerometers tested during the experimental tests are low-cost sensors that are activated only if the recorded acceleration exceeds a certain threshold. The choice of using low-cost accelerometrs is related to the possibility of using them in full scale buildings, combining the needs of accuracy and costs. Moreover, since the roof floor is considered as a rigid plane, the number of sensors is considerably reduced. Consequently, bi-directional accelerometers and the inclinometer can be integrated on top and at the bottom of one column within the building.

3 THE CASE STUDY

3.1 Description of the structure

A single-story precast RC industrial building with a rectangular floor plan (32.16 m x 18 m) is chosen as a case study (Figure 2).

The structure is located in a seismic area about 20 km far from Perugia, in central Italy. The structural scheme, which is typical for RC precast industrial structures, is constituted by a grid of 8 isostatic columns (0.5 m x 0.5 m x 6 m) indicated as C1-C8 in Figure 2, prestressed principal I-shaped beams pinned to the columns, roof elements pinned to the beams and vertical cladding panels connected to the beams. The foundation consists of plinths linked by a reinforced concrete slab, as at the ground level there is a RC industrial floor.

3.2 The finite element model

Starting from the building design documentation (specifications, technical

drawings, instructions and other relevant documents), a FEM of the building is reconstructed in SAP2000 (CSI) and used to apply the methodology described in Section 2.1.

Columns are beam elements with fixed joints at the base and are connected with the prestressed RC beams through hinge joints. The longitudinal beams are loaded with additional masses in order to account for the presence of the external infills.
The first mode (Φ_y) is flexural in *y* direction (transversal) with a small torsional component, the

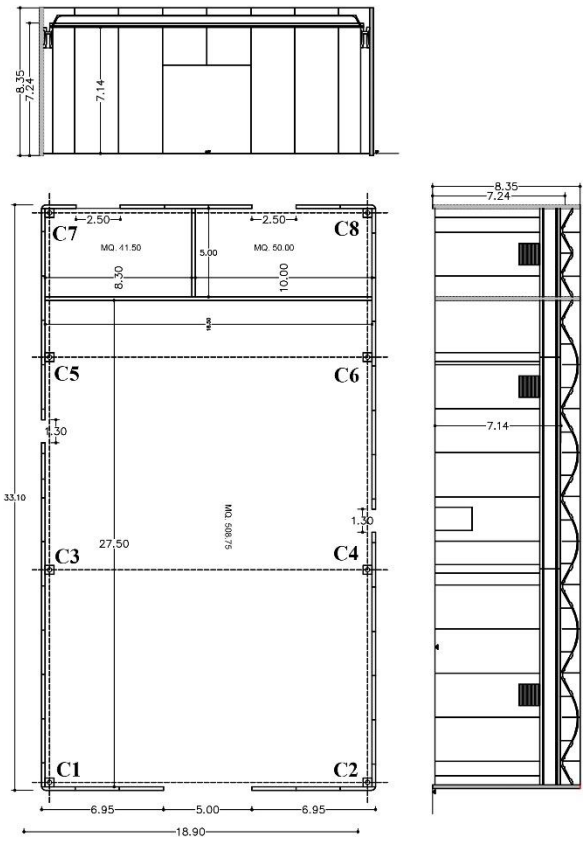

Figure 2: Plan view of the case study building with the corresponding front views.

second mode is purely flexural in *x* direction (Φ_x) and the third mode is torsional (Φ_z).
Table 1 summarizes the main modal characteristics of the analyzed structure. The effect of the vertical panels on the structural stiffness is neglected at this stage of the work.

Table 1. Main modal characteristics of the analyzed building.

Mode no.	*f* (Hz)	Mode shape	Modal participating mass ratios		
			x	*y*	*z*
1	0.582	Φ_y	0	0.995	0.077
2	0.584	Φ_x	1	0	0
3	0.832	Φ_z	0	0.005	0.995

In order to reproduce the nonlinear behavior of the structure, plastic flexural hinges are assigned at the base of each column, where cracking is expected as the flexural displacement approaches the ultimate strength. Hinges are modeled in SAP2000 according to the prescriptions available in ATC-40. Hence, the M-θ elastoplastic curves are reconstructed in five reference points A, B, C, D, E (Figure 3): the segment AB represents the linear elastic range; the point B refers to the yielding conditions M_y-θ_y; the point C refers to the ultimate conditions M_u-θ_u; the point D M_{u*}-θ_u refers to the ultimate curvature corresponding to a reduction of M_u equal to 80%, determined from the moment–curvature analysis; the point E M_{u*}-θ_{u*} is taken as θ_{u*}=1.5θ_u. The confined concrete stress–strain model is included in the nonlinear constitutive law (EN 1998-1 2004).

The plastic hinges non-linear states can be defined as: Immediate Occupancy (IO), Life Safety (LS) and Collapse Prevention (CP). For this numerical application, these states are included by dividing the B-C segment into four parts (Inel and Ozmen, 2006) delimited by IO (10% of B-C,) 60%, and 90%, LS (60% of B-C,) and CP (90% of B-C).

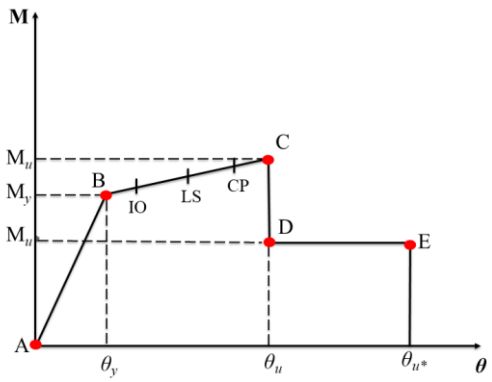

Figure 3: M-θ relationship of a plastic hinge.

3.3 The analysis cases

In order to account for the probabilistic nature of the seismic hazard, the NLSA are carried out considering different features, for a total of 60 analysis cases:

- three positions of the control joint at which the pushover curve is monitored (elastic center of the roof and top of the columns on the opposite building's corners);
- five positions of the accidental mass eccentricity (the geometric center and +- 5%

from the geometric center on each side of the building);
- two lateral forces distributions: proportional to the vibration mode and proportional to the mass distribution;
- two directions of the load (principal directions of the building with positive and negative sign of the load);

To perform NLDA, a set of 7 double-component (*x*,*y*) spectrum-compatible accelerograms are generated using the software Rexel (Iervolino et al. 2010), according to the Eurocode 8 (EN 1998-1 2004). Figures 4a)-b) show the 7 accelerograms' time histories for each main direction and Figures 5a)-b) present the corresponding spectra.

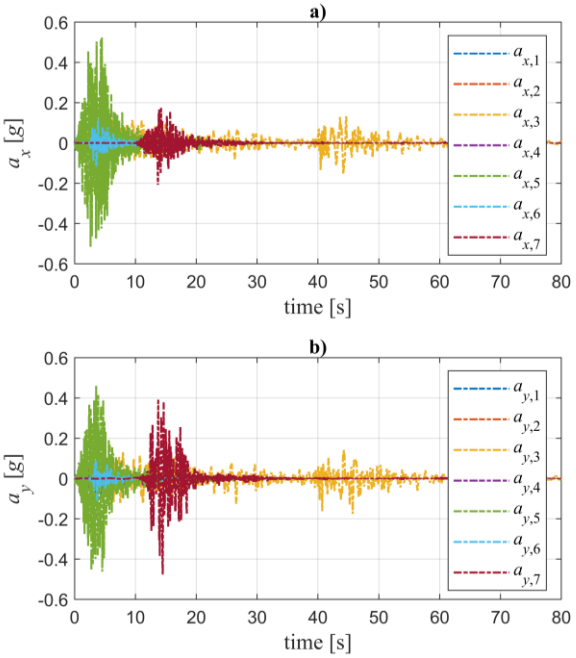

Figure 4. Set of accelerograms time histories: a) *x* direction; b) *y* direction.

The NLDA are repeated for a total of 70 analysis cases:
- for the seven double-component accelerograms;
- reversing the direction of application of the first component of the accelerogram (in the x direction and in the y direction);
- considering five positions of the accidental mass eccentricity; no eccentricity, + and - 5% of the corresponding building's side in both *x* and *y* directions.

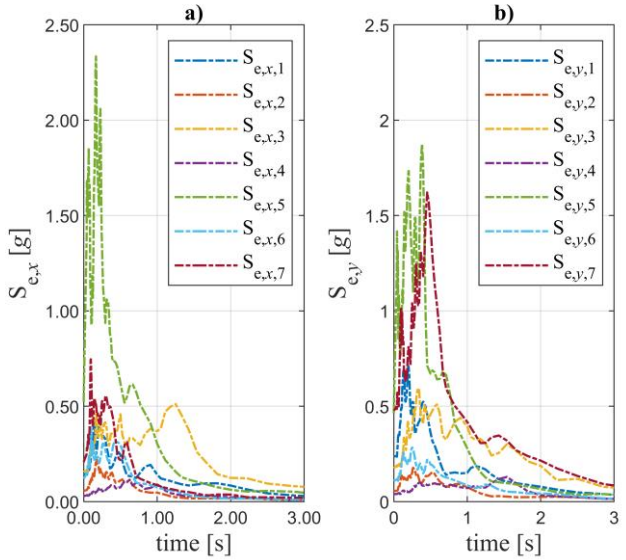

Figure 5. Set of accelerograms elastic spectra: a) x direction; b) y direction.

4 NUMERICAL RESULTS

4.1 Results of NLSA

The pushover curves resulting from the NLSA relate the base shear to the displacement of the control joint. Figures 6 a)-b) illustrate the pushover curves obtained for the *x* and *y* directions when the control point is the building's corner, i.e., top of C8 column in Figure 2.

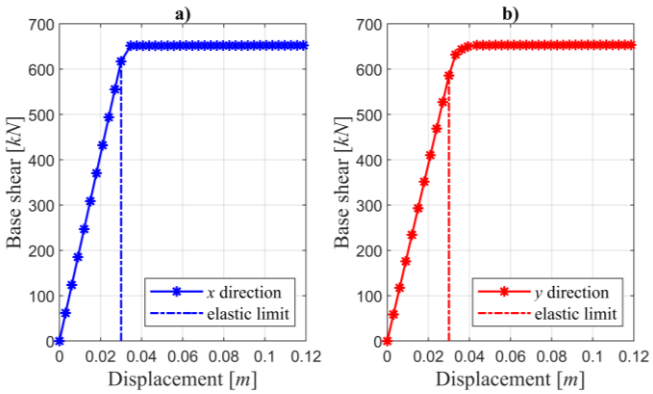

Figure 6. NLSA pushover curves: a) *x* direction; b) *y* direction

For the specific case study, the curve is linear elastic until the formation of the first plastic hinge representative of point B (Figure 3) and, beyond this step, the system is subjected to plastic deformation. In the *y* direction (shorter side of the building) all the plastic hinges are formed

simultaneously at the base of the columns at step 11. In the *x* direction the plastic hinges are coupled to the base of the two parallel columns starting from one lateral side and they develop from step 11 to 14 to the other building's columns. Thus, considering the different mass distribution on the building of the structural and nonstructural elements along the two principal directions, the structure in the y direction is most affected by torsional effects.

4.2 Results of NLDA

From the results of the NLDA the value of the displacement at the top of the column that first reaches the plastic hinge (at the base) is selected. As an example, Figures 7 a)-b) show the evolution in time of the displacement at the top of the column located at the building's corner in the *x* direction for accelerograms 1 and 3 with the indication of the time instant t_h when the plastic hinge is formed.

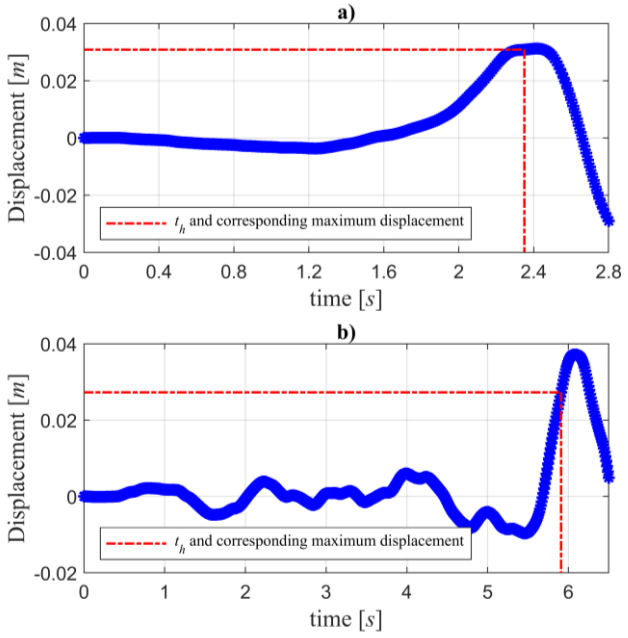

Figure 7. Time histories of the NLDA displacements at the top of the column located in the building's corner in the *x* direction with the indication of the time instant t_h when the plastic hinge is formed: a) accelerogram 1; b) accelerogram 3.

From the NLDA results it can be deduced that the plastic hinges are coupled to the base of the two parallel columns in the *y* direction starting from one of the external side of the building.

4.3 Results comparison

The mean value and standard deviation of the top displacements corresponding to the first elastic hinge formation obtained from all the analysis cases of both NLSA and NLDA are adopted to evaluate the corresponding CDF according to a Gaussian distribution. Each point of the CDF curves represents the probability of plastic hinge activation conditional on a specific value of IDR, characterizing the vulnerability of the structure.
Figure 8 shows the two CDFs of displacement corresponding to the elastic limit state exceedance and the corresponding area (grey filled area) where the on-off control alert is activated. From the figure can be highlighted that NLSA results are more conservative (lower values of IDR) then the NLDA. On the other hand, the uncertainty level associated to NLSA turns out to be more pronounced, causing a larger interval of IDRs at which the AL is switched on.
Hence, despite an high computational cost, NLDA has the potential to provide more accurate information for predicting the amount of damage, and consequently for assessing damage risk.

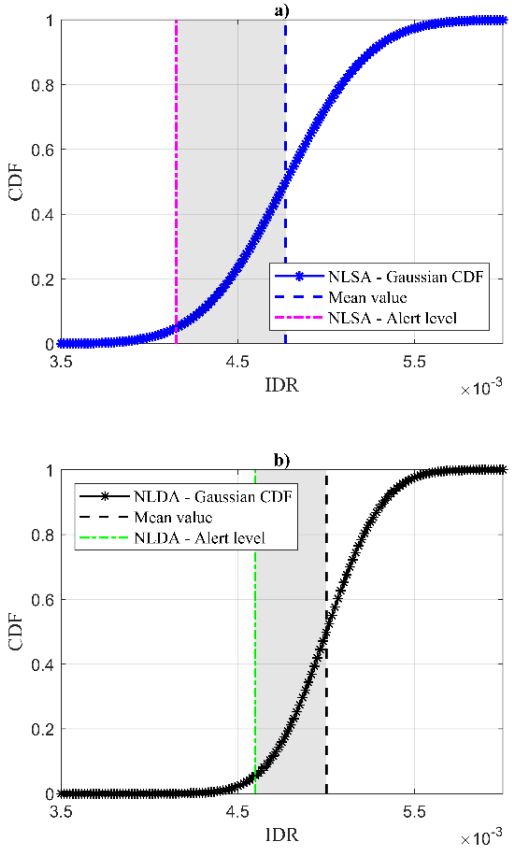

Figure 8. Gaussian CDFs conditional on IDR considering: a) NLSA results; b) NLDA results.

A larger value of standard deviation is probably expected in the case of more complex geometries and by adding sources of uncertainties related to structural parameters. Indeed, it is noteworthy that the procedure is general and allows to include different uncertainties in the analysis, like those associated to the bars corrosion or to the behavior of the connection joints between the structural elements or between structural and nonstructural elements.

4.4 Long-term monitoring simulation

With the main objective of validating the proposed methodology, a numerical analysis is carried out by simulating an online monitoring activity during an earthquake. Thus, a linear dynamic analysis is performed on the FEM by using the real seismic sequence occurred on October 30th 2016 and recorded by the INGV (National Institute of Geophysics and Volcanology), station FCC (Forca Canapine). Since the location of FCC is at a distance of about 130 Km from the case study building, the acceloragram is suitably scaled according to Bindi et *al*. 2009, in order to account for the epicentral distance.

Figure 9 shows the DI over time evaluated according to Eq. (2).

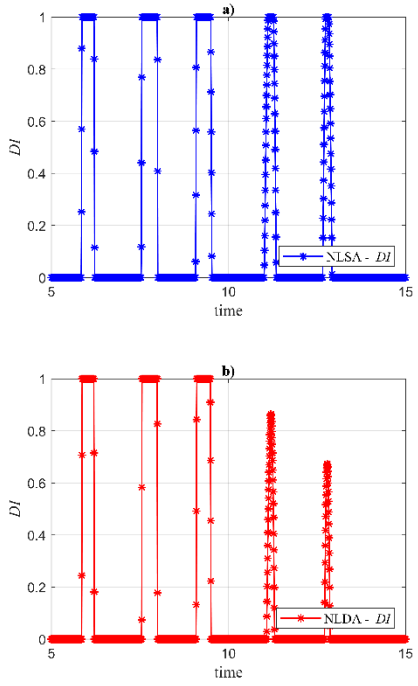

Figure 9. DI over time: a) NLSA results; b) NLDA results.

It can be noted that *DI* reaches the maximum allowable value in a few time steps during the seismic event. This index, associated with the residual drift measurements and the consequent visual inspection, could give an indication on the post-earthquake safety level of the structure.

It is worth noticing that the response of the FEM may be sensitive to the strengths and stiffnesses of its components and the actual properties may not be known accurately and the results illustrated in Figure 9 have the main objective of highlighting the potential of the proposed procedure in getting information for making decisions, not to predict the exact behavior of the structure.

5 CONCLUSIONS

This paper presents a general methodology based on long term monitoring data for the post-earthquake diagnosis of precast reinforced concrete buildings. An easily understandable decision parameter, DI, is used to quantify the possible damage and to make decision on the structural safety.

The effectiveness of the methodology is demonstrated by making use of a real single-floor precast reinforced concrete structure. Low-cost sensors are experimentally tested with the main goal of using them in full scale buildings, combining the antithetical needs of benefits and costs.

NLSA and NLDA are performed on a FEM for reproducing the dynamic behavior of the structure. The results of NLSA and NLDA are processed in a probabilistic manner, enabling the definition of alert levels and the inclusion of performance-based concepts.

The comparison between results of NLSA and NLDA highlights that the NLDA lead to a more reliable and robust results.

The proposed approach is general and could be easily applied to different cases studies. Moreover, different sources of limit states, like those associated to bars corrosion or connections between structural and nonstructural elements, can be readily included in the probabilistic-based methodology.

6 ACKNOWLEDGMENT

The project is funded by the European social fund in the framework of POR FESR - Axis 8 - Seismic prevention and support for the recovery of the areas affected by the earthquake. The Authors would like to acknowledge the support of Manini Prefabbricati s.p.a, Santa Maria degli Angeli, Perugia (Italy), for the support and collaboration on the research activity.

REFERENCES

ATC-40, Applied Technology Council, Seismic evaluation and retrofit of concrete buildings, vol. 1 and 2, California; 1996.

Belleri, A., Moaveni, B., Babuska, I., Restrepo, J.I., 2014. Damage assessment through structural identification of a three-story large-scale precast concrete structure, *Earthquake Engineering and Structural* Dynamics, **43**, 61–76.

Bindi, D., Luzi, L., Pacor, F., Sabetta, F., Massa, M., 2009. Towards a new reference ground motion prediction equation for Italy: update of the Sabetta–Pugliese (1996). *Bulletin of Earthquake Enginering*, **7**(3), 591–608.

Brunesi, E., Nascimbene, R., 2017. Experimental and numerical investigation of the seismic response of precast wall connections, *Bulletin of Earthquake Enginering*,15, 5511-5550

CSI, SAP2000 Integrated Software for Structural Analysis and Design, Computers and Structures Inc., Berkeley, California.

EN 1998-1, Eurocode 8, 2004. Design of Structures for Earthquake Resistance. 1st ed. Brussels: BSi.

Graham, H. P. and Rakesh, A., 1988. Seismic damage prediction by deterministic methods: Concepts and procedures, *Earthquake Engineering and Structural Dynamics*, **16**, 719–734.

Ierimonti, L., Caracoglia, L., Venanzi, I., Materazzi, A.L., 2017. Investigation on life-cycle damage cost of wind-excited tall buildings considering directionality effects, *Journal of Wind Engineering and Industrial Aerodynamics*, **171**, 207–218.

Iervolino, I., Galasso, C., Cosenza, E., 2010. REXEL: Computer aided record selection for code- based seismic structural analysis, *Bulletin of Earthquake Engineering*, **8**(2), 339–362.

Inel, M., Ozmen, H.B., 2006, Effects of plastic hinge properties in nonlinear analysis of reinforced concrete buildings, *Engineering Structures*, **28**, 1494–1502.

Isidori, D., Concettoni, E., Cristalli, C., Soria, L. Lenci, S., 2016. Proof of concept of the structural health monitoring of framed structures by a novel combined experimental and theoretical approach, *Structural Control And Health Monitoring*, **23**, 802-824.

Liberatore, L., Sorrentinp, L., Liberatore D., Decanini D. L., 2013. Failure of industrial structures induced by the Emilia (Italy), *Engineering Failure Analysis*, **34**, 629-647).

Pierdicca, A., Clementi, F., Maracci, D., Isidori, D., Lenci, S., 2016. Damage detection in a precast structure subjected to an earthquake: A numerical approach, *Engineering Structures*, **127**, 447–458.

Rave-Arango, J.F., Blandón, C.A., Restrepo, J.I., Carmona, F., 2018. Seismic performance of precast concrete column-to-column lap-splice connections, *Engineering Structures*, **176**, 687-699.

Senel S.M., Kayhan A.H., 2010. Fragility based damage assesment in existing precast industrial buildings: A case study for Turkey, *Structural Engineering and Mechanics*, **34**(1),39-60.

Ubertini, F., Cavalagli, N., Kita, A., Comanducci, G., 2018. Assessment of a monumental masonry bell-tower after 2016 Central Italy seismic sequence by long-term SHM, *Bulletin of Earthquake Engineering*, **16**, 775–801.

Guo, G., Zhai, Z., Cui, Y., Yu, Z., Wu, X., 2019. Seismic performance assessment of low-rise precast wall panel structure with bolt connections, *Engineering Structures*, **18**, 562-578.